CMLS, Cell. Mol. Life Sci. 58 (2001) 1451–1460
1420-682X/01/101451-10 $ 1.50 + 0.20/0


**CMLS Cellular and Molecular Life Sciences**

# Review

# Superefficient enzymes

**M. E. Stroppolo, M. Falconi, A. M. Caccuri and A. Desideri***

INFM and Department of Biology, University of Rome 'Tor Vergata', Via della Ricerca Scientifica, 00133 Rome (Italy), Fax: +39 06 7259 4326, e-mail: desideri@uniroma2.it

Received 29 January 2001; received after revision 23 March 2001; accepted 19 April 2001

**Abstract.** Diffusion-controlled enzymes are characterized by second-order rate constants in the range $10^8$–$10^{10}$ $M^{-1}s^{-1}$. These values are at the upper end of the observed rates of many enzyme-substrate reactions and have been predicted by theoretical studies on bimolecular reaction in solution. Such enzymes are considered to be perfect, since their rate-limiting step is not due to any chemical event but to the diffusional association rate between the enzyme and the substrate. Often the enzyme-substrate encounter is facilitated either through the presence of a strong attractive electric field, produced by charges on the enzyme surface, or through the reduction in the dimension of the search process. Here we provide a brief review of some of the enzymes characterized by a very fast second-order constant, focusing attention on triose phosphate isomerase and Cu,Zn superoxide dismutase taken as typical examples of such highly tuned enzymes.

**Key words**. Electrostatics; Brownian dynamics; diffusion control; triose phosphate isomerase; Cu,Zn superoxide dismutase.

## Introduction

Any enzymatic reaction can be divided as a first approximation into two steps: the first concerns the encounter between the enzyme and the substrate and is mainly determined by physical factors; the second one depends on the appropriate structural and dynamical arrangement of the enzyme lateral chains and is determined by chemical factors.

Enzymes characterized by extremely efficient reaction rates are supposed to be perfect from a chemical point of view, so the rate-determining step for their second-order catalytic rate corresponds to the association of the free enzyme and the free substrate. In these cases the second-order catalytic rate may be as high as $10^{10}$ $M^{-1}s^{-1}$ and is never lower than $10^7$ $M^{-1}s^{-1}$. The degree to which an enzyme reaches the diffusion limit gives some measure of how far an enzyme has evolved. The diffusion-limited encounter of molecules in solution can be calculated by the Einstein-Smoluchowski equation [1]. Such a rate, for two proteins approximated to spheres of 18 Å radius which associate with every contact without regard to orientation, is equal to $7 \cdot 10^9$ $M^{-1}s^{-1}$. The orientational constrains, due to steric specificity when the proteins associate, reduce the association rate constant by up to three orders of magnitude [2]. Nevertheless, very high rate constants can be found for reactions between macromolecules. High association rate constants have been found for the association of barnase and barstar [3], of hirudin and thrombin [4], ferricytochrome c and ferrocytochrome $b_5$ or in the association of the protein-DNA [5] or protein-substrate [6] complex.

Enhancement of the association rate is achieved by facilitated diffusion obtained either through the presence of strong attractive coulombic forces [7] or through reduction of the encounter process from a three-dimensional (3D) random search to a monodimensional mechanism [8]. A reduction in the dimension of the search process has been proposed in the formation of many protein-DNA complexes and implies nonspecific binding to any point

* Corresponding author.

on the DNA followed by movement along the DNA until the target sequence is located or the protein dissociates. The effective target size of the DNA is increased compared with a single binding event, enhancing the association rate constant for specific binding. One-dimensional facilitated diffusion has been reported for several proteins that interact with DNA such as the lac repressor [9], EcoRI endonuclease [10], RNA polymerase [11], BamHI endonuclease [12], T4 endonuclease V [13] and the T4 late enhancer complex [14]. More recently, facilitated diffusion in one dimension along a single-strand nucleic acid has been also reported for a ribonuclease [15]. In this latter case the diffusion is also mediated by coulombic interactions since the effect is diminished by the addition of NaCl. In the case of EcoRI methyltransferase it was possible to correlate the catalytic constants $k_{cat}$ and $k_M$ to DNA length and specific site location within the DNA molecule [16]. In fact, the $k_{cat}/k_M$, which was found to be $5.1 \cdot 10^7$ $M^{-1}s^{-1}$ for a 14-bp DNA substrate, undergoes a fourfold increase for a 429-bp DNA substrate and increases twofold as the distance from the site to the nearest end is increased from 29 to 378 bp.

The presence of a strong attractive electrostatic field can also enhance the enzyme-substrate encounter. In this case it is possible to calculate the enzyme-substrate association rate, which as a first approximation is equal to the enzyme catalytic rate, by evaluating the diffusion of the substrate forced by the presence of the electric field produced by the enzyme. This is done by simulating Brownian dynamics to evaluate the probability of the active site-substrate encounter over an ensemble of $10^4$ different trajectories. A trajectory is normally initiated by placing the substrate at a distance of 60–70 Å from the active site and continues until it enters a sphere of radius 4–5 Å centered on the active site or escapes by reaching a sphere of 150–160 Å from the protein center. The method permits evaluation of the effect on the substrate-enzyme probability encounter due to the electric field variation because of mutations of charged residues. Here we will discuss in detail the case of triose phosphate isomerase (TIM) and Cu,Zn superoxide dismutase (SOD), although the same electrostatic facilitated diffusion has been claimed for many enzymes, such as acetylcholinesterase and $\beta$-lactamase, and to describe the formation of the barnase-barstar complex.

In the case of acetylcholinesterase, evidence for a diffusion-controlled reaction was provided upon investigating the substrate association rate constant in glycerol/water solvents of increased viscosity [17]. Confirmation that electrostatic attraction is the driving force for rapid enzyme-substrate binding comes from the ionic strength dependence of the association rate between acetylcholinesterase and *N*-methyl acridinium or acetylthiocholine [18]. An uneven spatial charge distribution was observed in the structure of *Torpedo californica* acetylcholinesterase [19], and these electrostatic properties were proposed to play an important role in attracting the positively charged substrate and in steering it toward the active center gorge of the enzyme [20]. Unexpectedly, a large number of mutations of charged residues were shown to have little effect on the rate of substrate binding [21]. This result was interpreted as evidence for a lack of diffusion control and electrostatic steering. However, the rates of the mutants could be well reproduced through simulating Brownian dynamics, which demonstrate enhanced of rates because of electrostatic steering of substrate toward and inside the substrate binding gorge [22–23].

$\beta$-Lactamases have been characterized as fully efficient enzymes with no single rate-determining step [24]; they are partly diffusion-controlled for good substrates such as benzylpenicillin with a single negative charge, and most have catalytic rates of $10^7$–$10^8$ $M^{-1}s^{-1}$ for such substrates at 10 mM ionic strength [25]. Analysis of the electrostatic potential of different natural variants of this class of enzymes indicated the presence of a conserved positive potential along the active site cleft which is mainly due to Lys234 and Arg244 [26]. Lys234 is conserved in most known sequences and is conservatively substituted by an Arg residue in enzymes which efficiently hydrolyze $\alpha$-carboxypenicillins [27–28]. Crystallographic data indicate that the side chain of Lys234 points into the active site, and Herzberg and Moult [29] first suggested that its protonated amino group participates in binding the substrate. An Arg is present at position 244 in 15 of the 20 sequences aligned by Ambler et al. [30]. No Arg was found in *Symphoricarpos albus* lactamase, but comparison of the 3D structure indicated that in this case a new Arg in position 220 is present whose guanido group occupies a position very similar to that of Arg244 in the other enzymes. Lys234, Arg220 and Arg244 have been the subject of mutational studies in several $\beta$-lactamases [25]. These studies have shown that Lys234 plays a role in both initial recognition of the substrates and in stabilizing the transition state. Mutation to a nonpolar residue of Arg244 or Arg220 in the corresponding protein had a deleterious effect on the catalytic rate for charged substrates and indicated their important role for the substrate binding.

A case of a very fast enzyme-inhibitor association rate is represented by the ribonuclease barnase. The association between barnase and its natural intracellular inhibitor barstar is in fact $5 \cdot 10^9$ $M^{-1}s^{-1}$ [31] and even so the rate of binding could be improved by mutation [32]. Mutation of charged residues and modulation of the ionic strength indicated that the association process can be divided into two phases. In the first phase the two proteins form a low-affinity nonspecific complex which is held together by long-range electrostatic interactions. The extent of freedom in this complex is dictated by the magnitude of the electrostatic interaction. The higher the favourable elec-

trostatic forces between the proteins, the less specific the transition state and the higher the reaction rate. The second phase is the docking of the two proteins to give the final high-affinity complex. The effect of mutation and ionic strength on the association rate could be well reproduced by simulating Brownian dynamics, confirming the role of electrostatic field in modulating the association rate [33].

## TIM

A well-characterized example of a diffusion-controlled enzyme is represented by TIM, which mediates protonation and deprotonation for the interconversion between dihydroxyacetone phosphate (DHAP) and glyceraldehyde 3-phosphate (GAP). The TIM enzyme has been described as a perfect enzyme because its rate-determining step is not the chemical event or any conformational step occurring during catalysis but the diffusional association of substrate and enzyme. In the presence of viscosogenic agents such as sucrose and glycerol, the plot of the reciprocal of the relative values of $k_{cat}/k_M$ against the relative viscosity gives slopes close to unity, as predicted by the Stokes-Einstein equation, indicating a diffusion-limited catalyzed reaction [34].

The TIM catalytic mechanism may be summarized as follows (fig. 1): binding of the substrate DHAP; abstraction by a general base of the pro-R proton at C1 of the substrate, yielding the cis-enediolate intermediate; protonation of the enediolate species at C2 by a general acid to yield the product GAP. The conserved active-site residue, Glu165, is recognized as the general base responsible for the pro-R proton capture at C1 of the substrate DHAP or, in the reverse reaction, of the proton at C2 of GAP. An important role is played by His95, which shuttles a proton between the two oxygen atoms of the enediolate intermediates [35]. A computer simulation study, carried out by Åqvist et al. [36], evaluated the complete free-energy profile for all the elementary steps of the TIM-catalyzed reaction using simulation of molecular dynamics free-energy perturbation in combination with the empirical valence bond method. The resulting free-energy profile of the catalyzed reaction shows all intermediates to be stabilized when compared with those of the uncatalyzed reaction. The authors suggest that the efficient catalytic mechanism of TIM can be achieved both by lowering the energies of charged intermediates through several hydrogen bonds and by reduction of the reorganization energies, due to the perfect orientation of the dipoles in the active site. The relative position of the Glu165 residue and the substrate appears perfect because of the short distance (3.4 Å) from the carboxylate and the substrate, which requires minimal motion to remove the proton from C1 of DHAP or from C2 of GAP. When Glu165 is mutated into Asp, the distance between the base and the substrate

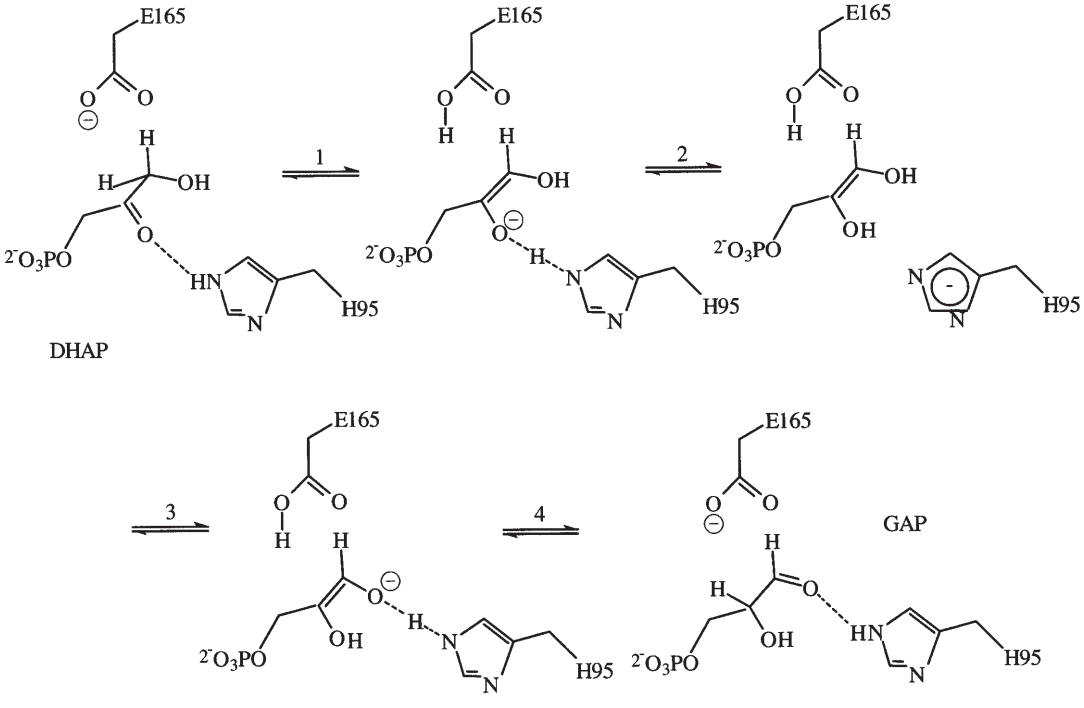


Figure 1. Schematic mechanism of TIM reaction. Substrate DHAP binds to the TIM active site, E165 abstracts the proton at C1 of the substrate, the cis-enediolate intermediate is obtained, H95 shuttles a proton between the two oxygen atoms of the enediolate intermediates, protonation of the enediolate species at C2 by E165 leads to the product GAP. The low-barrier hydrogen bonds between the enediol and neutral imidazole are represented by (–H–), whereas the usual hydrogen bonds are represented by a dashed line.

varies by approximately 1 Å, and the rate of catalysis slows down of about a thousandfold [37]. The enzyme also uses electrophilic catalysis through the imidazole ring of His95, which is crucial in polarizing the substrate carbonyl groups and shuttles protons between the oxygen of the two enediolate intermediates. Mutation of His 95 residue to Gln or Asn results in a 100 and $10^4$ times less active enzyme, respectively [38].

Recently, a clear demonstration was shown of the role played in the TIM catalysis by low-barrier hydrogen bonds (LBHBs) [39–41], where the hydrogen is shared between a donor and acceptor having similar p*K,* and the interaction between the hydrogen and both of them is considered to be almost covalent. When an enzyme active site closes around the substrate, excluding the solvent, the effective dielectric constant is close to that observed in organic solvent, and a weak hydrogen bond may be converted into a LBHB in the transition state. In the reaction catalyzed by TIM, a ketone of the substrate is hydrogen-bonded to the neutral imidazole ring of His95. When Glu165 removes a proton from the substrate and the enediolate intermediate is formed, its p*K* matches the p*K* of neutral imidazole, and the resulting LBHB between one oxygen of the enediolate intermediate and neutral His95 (fig.1) provides much of the energy needed to speed up the enolization of the substrate.

Simulation studies have proposed that in TIM a crucial role in catalysis may be also played by an active-site water molecule trapped between Glu165 and His95, which stabilizes the negative charges formed during catalysis [42]. A recent X-ray diffraction study identified the presence of well-defined water molecules in the TIM active site involved in an extensive hydrogen-bonding network that may lock the side chain of Glu165 down on the substrate in the correct orientation [43].

Beside these structural features, other aspects contribute to the highly efficient catalysis of this enzyme, such as electrostatic steering of the substrate toward the active site. Wade et al. carried out simulations of Brownian dynamics on the association of GAP with TIMs from four species with net charges at pH 7.0 between –12*e* and +12*e* [44]. Despite the wide variation in net charge, the rates of these enzymes show only modest differences. From the analysis of Brownian dynamics it appears that two highly conserved regions of positive potential are clearly discernible around the active sites and attract the negatively charged substrate into the active sites. This conserved positive potential is in part due to the conservation of two lysine residues in all four TIMs: the catalytic Lys13 in the active site and Lys237 more than 10 Å distant from Lys13. Nuclear magnetic resonance (NMR) experiments have also shown that the internal dynamics of a flexible loop of 11 amino acids (residues 166–176) is on the time scale of catalytic turnover, but the loop closure is not triggered by binding of substrate or product. The loop is constantly opening and closing, and enolization only occurs when the lid is closed [45]. Mutagenesis studies [46] showed that in the absence of a proper lid, the enediol phosphate intermediate is lost from the mutated enzyme into the solution and decomposes rapidly into methylglyoxal and inorganic phosphate. The flexible loop closure constrains the intermediate on the surface of the enzyme in a conformation unfavourable for its elimination, and separates the intermediate from solvent, thus lowering the energy required for enolization. The speed of loop closure is also important; mutation of three amino acids at the C-terminal hinge of the loop results in a slower loop closure or steric hindrance, and the Michaelis complex formation becomes rate limiting in catalysis [47].

## Cu,Zn SOD

Cu,Zn SODs build a class of ubiquitous metalloenzymes which catalyze the dismutation of the superoxide radical anion into oxygen and hydrogen peroxide [48–51], according to the schematic reaction:

$$2\ O_2^- + 2\ H^+ \rightarrow H_2O_2 + O_2$$

The dismutation reaction involves successive encounters of two distinct superoxide anions with the enzyme catalytic center [in the Cu(II) and Cu(I) oxidation states, respectively], which is hosted at the surface of the enzyme Greek-Key $\beta$ barrel, at the dead end of a narrow protein channel (see fig. 2). In the eukaryotic enzyme the copper site is coordinated to four invariant histidine residues (atom ND1 of His 44 and atoms NE2 of His 46, His 61 and His 118) whereas the zinc ion is coordinated by one Asp and three His residues (atoms ND1 of His61, His69, His78 and OD1 of Asp81 (fig. 3). Also Cu,Zn SODs are usually described as perfect enzymes with second-order catalytic rates ($k_{cat}/k_M$) of the order of $10^{-9}$ $M^{-1}s^{-1}$. The dismutation reaction of SOD can be described by the following scheme [6]:

$$SOD + O_2^- \underset{k_{-1}}{\overset{k_1}{\longleftrightarrow}} O_2^- - SOD \xrightarrow{k_2} \text{products}$$

where $k_1$ is the second-order association rate constant, $k_{-1}$ is the first-order enzyme-substrate dissociation rate constant and $k_2$ is the first-order rate constant for the formation of products. These quantities are related in the Michaelis-Menten model for the enzyme kinetics by the following equation:

$$k_f = k_2/k_M = k_1k_2/(k_{-1} + k_2)$$

where $k_f$ is the second apparent order enzyme rate constant and $k_M$ is the Michaelis-Menten constant. In the case of SOD the catalytic process is diffusion limited, i.e. $k_f = k_1$, since $k_2 \gg k_{-1}$. Efficient superoxide dismutation is pro-

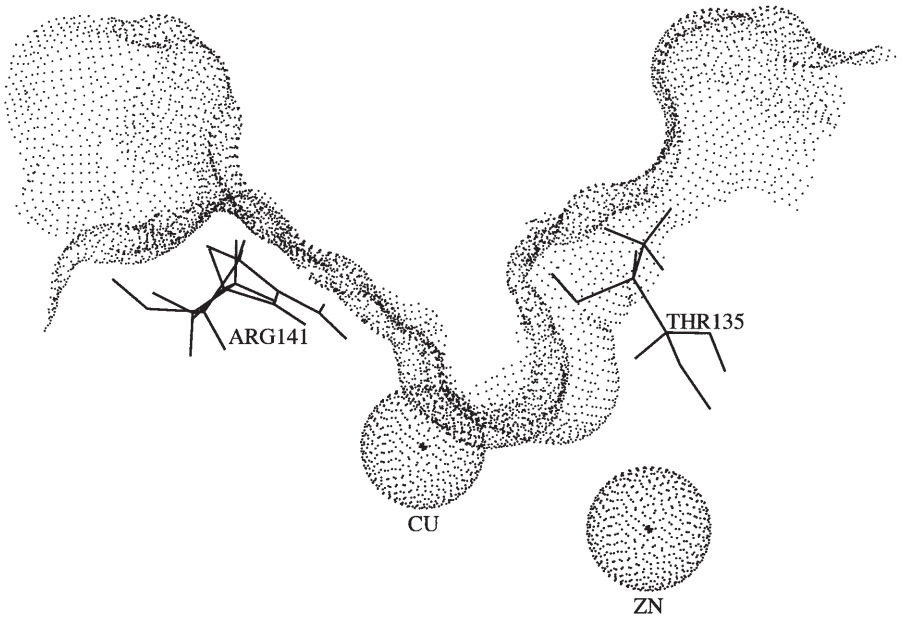


Figure 2. Cross section of the SOD active site. The diameter of the channel decreases stepwise toward the catalytic copper. Mobility of the residues Arg141 and Thr135, forming the sides of the channel, can increase or decrease the availability of the copper ion for the interaction with the superoxide. This picture was generated using version 6.2 of the SYBYL program (Tripos Inc., 1699 South Hanley Road St. Louis, Mo, 63144, USA).

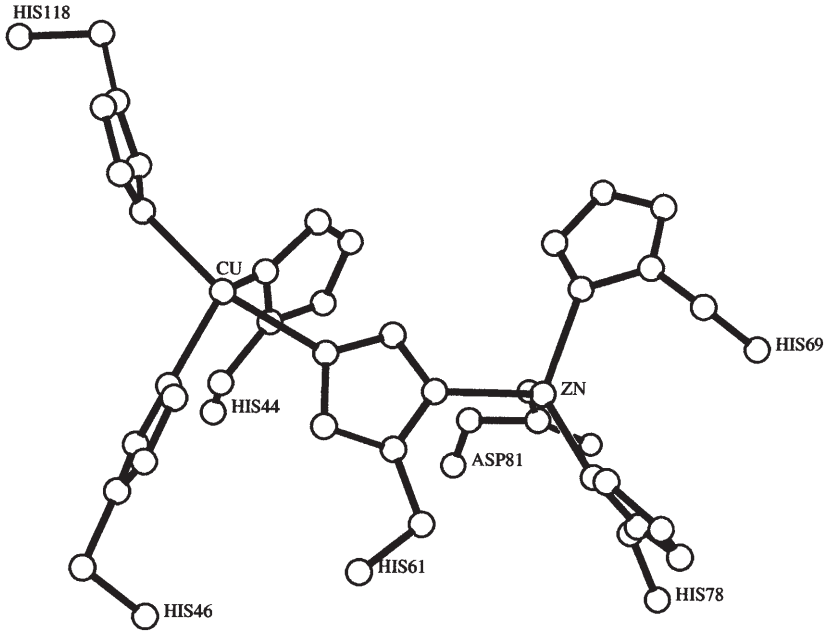


Figure 3. Geometry of the active site metal ligands viewed from the solvent. The Cu ligand form a tetrahedrally distorted square plane, whereas the Zn ligand forms a tetrahedral geometry with a distortion toward a trigonal pyramid with Asp81 at the apex. The side chain of His61 forms a bridge between the Cu and the Zn ions. This picture was generated using version 6.2 of the SYBYL program.

vided by the metal cluster and by a conserved Arg141 proximal to the active site. The chemistry of the reaction consists of two semireactions which describe the interaction of $O_2^-$ with copper in the oxidized and reduced states, respectively (fig. 4). The first semireaction involves coordination of the superoxide to the oxidized copper center, likely simultaneous with displacement of the loosely copper-bound water molecule, assisted by the invariant Arg141 residue, which may hydrogen-bond the incoming $O_2^-$. Stabilization of the Cu(II)-coordinated superoxide anion may also involve ordered active-site water molecule(s). $O_2^-$ is supposed to be coordinated to the Cu(II) in

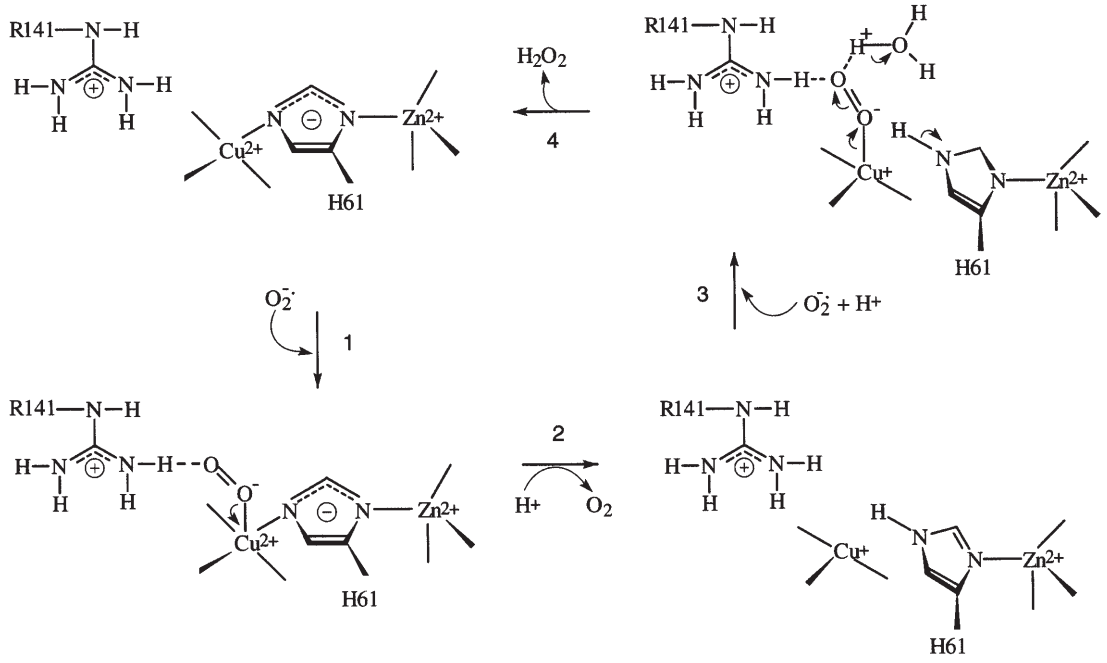


Figure 4. Schematic mechanism of Cu,Zn SOD reaction. $O_2^-$ displaces the axial $H_2O$ binding one O to the Cu(II) and hydrogen- bonding the second O to a guanidinium N of Arg141. Bound $O_2^-$ reduces the Cu(II) to Cu(I) with simultaneous breaking of the bond between His61 and the Cu; $O_2$ is released. His61 NE2 becomes protonated, ND1 remains bound to the Zn and the ring plane rotates out from the line joining the metals. Binding of a second $O_2^-$ to the Cu(I) places one O to hydrogen-bond with protonated His61 NE2, while the other O hydrogen bonds to Arg141. The Zn(II) bound to His61 ND1 raises the p$K_a$ of NE2, so unliganded NE2 will always be protonated at physiological pH. Addition of a second proton from an active site water gives the neutral $H_2O_2$ leaving group.

the equatorial plane, due to a lengthening of the His46 coordination bond (which becomes more axial), as suggested by the crystal structures of the complexes of Cu(II),Zn SODs from ox and yeast with azide and of the *Xenopus laevis* enzyme with cyanide [52, 53]. A redox event occurs via inner sphere electron transfer, from $O_2^-$ to Cu(II), yielding the neutral $O_2$ molecule and the reduced Cu(I),Zn SOD. The reaction product $O_2$ is no longer kept by electrostatic forces in the active site, and diffuses away, being replaced by a water molecule. As a result of reduction, the Cu(I) center adopts a trigonal coordination, based on His44, His46 and His118 ligands. Rupture of the coordination bond between copper and the NE2 atom of His61 (the bridging imidazolate) is concomitant with protonation of the imidazole ring and with a sizeable shift (ca. 1 Å) of the Cu(I) ion from its position in the oxidized enzyme.

In the second half-reaction, diffusion of a superoxide anion to the Cu(I) center is also driven by electrostatics, and may be supported by Arg141 hydrogen bonding and by the replacement of one active-site water molecule. However, Fourier transform infrared in this case (FTIR) evidence [54] suggests that direct coordination of $O_2^-$ to the Cu(I) center is not achieved, the anion reaching a specific binding site, about 3 Å from the Cu(I) center, hydrogen-bonded to the Arg141 guanidinium group. Reduction of the substrate would then be based on outer-sphere electron transfer from the trigonal Cu(I) center. The protons required for neutralization of the product (to yield the electrostatically neutral $H_2O_2$) are provided by the protonated His61 residue, and by the active-site network of water molecules. The coordination of the bridging imidazolate (His61) to the newly formed Cu(II) center, with achievement of a copper square planar coordination, completes the catalytic cycle.

The enzyme-substrate encounter is optimized by distribution of the electrostatic potential generated by the charged amino acid residues, which are negative all around the protein except in the proximity of the active site (fig. 5). Several experimental and simulation results indicate that the SOD-$O_2^-$ bimolecular reaction rate is increased by the electrostatic attraction between the reactants. The idea of electrostatic guidance for the negatively charged substrate is consistent with the large decrease in reaction rate observed upon increasing the ionic strength from 0 to 150 mM [55, 56], and can be rationalized by considering that although the bovine dimeric enzyme has an overall negative charge (–3.0*e* at pH 7.0), the active center is surrounded by a positive electrostatic potential. The distribution of the electrostatic potential around the protein was first studied by Koppenol [7] and Getzoff [57] by calculating pairwise additive coulombic potentials. A further improvement was obtained by an analysis carried out by Klapper [58], who considered a double di-

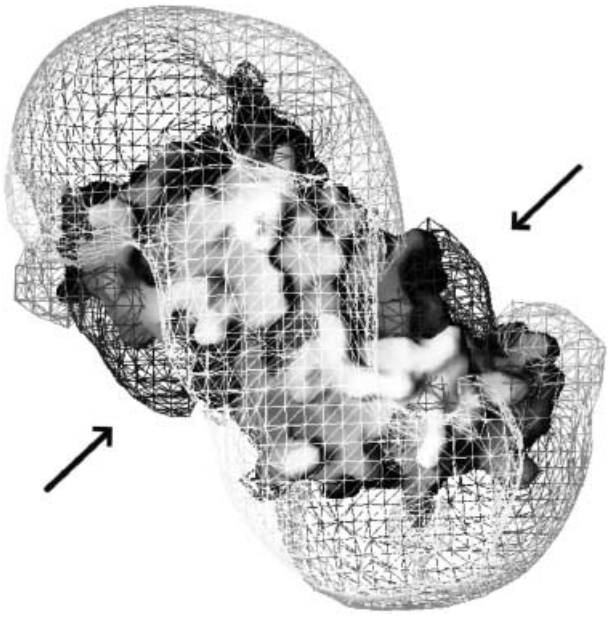

Figure 5. GRASP [80] 3D representation of the electrostatic potential field distribution around *bovine* Cu,Zn SOD. The dark grey network, surrounding the SOD catalytic sites indicated by arrows, represents the positive equipotential surface at 1.0 $kT/e$ (where $k$ is the Boltzmann constant, $T = 298$ K and $1kT/e = 0.0257$ V). The light grey network surrounding the rest of the protein represents the negative equipotential surface at –1.0 $kT/e$. The protein boundaries are shown by a rendered molecular surface. Equipotential surfaces in the protein interior are not drawn for clarity.

electric model, one for the protein and the other for the solvent, able to account for the negative salt dependence of the reaction rate. Subsequently electrostatic guidance for the enzyme-substrate interaction has been proposed to be related to a spatial distribution of charges, arranged to maintain in the area surrounding the active sites an identical electrostatic potential distribution which is conserved in the evolution of this protein family, irrespective of the protein net charge and conservation of single residues [59]. In line with this principle, different natural variants display almost identical second-order catalytic rates [60]. Simulations of Brownian dynamics have been able to reproduce the trend of the ionic strength dependency experimentally observed on the native and chemically modified bovine enzyme [61, 62], and to reproduce the experimental catalytic rate in six natural variants [6], indicating that this approach may be useful in order to estimate the role exerted by each charged residue in the enzyme-substrate encounter, and for engineering an enzyme with increased catalytic efficiency [63].

The first mutation aimed at understanding the role of the charged residues was engineered at site 141 [64], where a fully conserved Arg is located. This work, together with a subsequent, more extensive study [65], indicated that when Arg141 is substituted by Lys, which is still a positive residue but displays a different charge distribution, the enzyme loses part of its activity. The activity is reduced to 10% when Ile is present at site 141 and drops to 4% when a negatively charged residue is introduced. Brownian dynamics and mutagenesis were used to predict and produce superefficient mutants of the human enzyme that are more active than the wild-type enzyme [66]. In particular, substitution of the negative residues Glu131 and/or Glu130 with Gln produced a two to three-fold more active protein. However, electrostatics is not the only key factor, since the Glu131→Lys, Glu130→Gln mutant enzyme, which displays a further increase in local positive charge, is less active than the Glu131→Gln, Glu130SQ→Gln mutant, indicating that preorientation factors may also be relevant to correctly attract the substrate toward the active site. A similar increase in the catalytic rate has been observed in the Glu131→Gln mutant but not in the Asp130→Gln mutant of *Xenopus laevis* Cu,Zn SOD, indicating that residues occupying the same sequence position might have a different role in the Cu,Zn SODs from different organisms [67]. Lys120 and Lys134 residues have also been shown to play a role in the attraction of the superoxide substrate since their neutralization through site-directed mutagenesis yields mutant enzyme with activity lower than the wild type [67, 68]. It must, however, be stressed that residues Lys120, Asp130, Glu131 and Lys134 residing on the electrostatic loop have an important role in the electrostatic attraction of the substrate only at low ionic strength. In fact, the functional characterization of a quadruple Cu,Zn SOD mutant in which these residues are neutralized (Lys120 → Leu, Asp130 → Gln, Glu131 → Gln and Lys134 →Thr) has shown that at low ionic strength the mutant enzyme is more active than the wild type, whereas, at physiological ionic strength, the catalytic rate of the mutant is identical to that of the wild type, at any pH, indicating that an identical electrostatic attraction is felt by the substrate at each pH value [69]. At physiological ionic strength, the metal cluster and the invariant Arg141 are mainly responsible for the enhancement of the substrate diffusion toward the active site [69]. The ability of Brownian dynamics simulations to reproduce the experimental second-order catalytic rate confirms that the enzymatic reaction is diffusion limited because of a perfect architecture of the catalytic site, efficiently selected by nature to dismutate the superoxide anion.

The same mechanism also occurs in the prokaryotic Cu,Zn SODs, where diffusion enhancement of the substrate toward the active site is maintained despite modifications in their different tertiary and quaternary structures which displace the location of the electrostatic loop, as compared with eukaryotic enzymes [51, 70]. Actually, these structural differences make the copper more accessible to the external substrates, which permits the prokaryotic SODs to behave as superefficient enzymes when compared with eukaryotic ones. In fact, the recently

determined $k_{cat}/k_M$ for Cu,Zn SOD from *Photobacterium leiognahi* and *Salmonella typhimurium* is $8.5 \cdot 10^9$ and $1.3 \cdot 10^{10}$, respectively [71, 72], values higher than the value of $2 \cdot 10^9$ previously found for eukaryotic SODs [60]. Evidence for a substrate electrostatic attraction in prokaryotic Cu,Zn SODs comes from experiments which indicate that at low ionic strength, neutralization of Lys60 of the Cu,Zn SOD from *Escherichia coli* strongly reduces the catalytic activity of the enzyme (by ca. 50%), indicating that this residue plays a primary role in the electrostatic attraction of the substrate, whereas neutralization of Lys63 does not significantly influence the catalytic rate [73]. In the case of the prokaryotic enzyme from *P. leiognathi*, it has been possible to engineer a superefficient enzyme, by introducing the Glu59 →Gln mutation [74]. At neutral pH this mutant was found to have a $k_{cat}/k_M$ of $1 \cdot 10^{10}$ $M^{-1}s^{-1}$, likely due to a series of combined effects (such as an enhanced substrate attraction by the modified electrostatic field distribution, a large solvent-accessible active-site, a specific intersubunit interaction which may influence the active site arrangement). Remarkably, it has been observed that the catalytic efficiency of the prokaryotic enzyme can be modulated by mutation of residues located at the intersubunit interface [75]. This mutation gives rise to a superefficient mutant characterized by a $k_{cat}/k_M$ of $1.7 \cdot 10^{10}$ $M^{-1}s^{-1}$, the fastest rate ever found in any SOD, and demonstrates intramolecular communication between the mutation site and the catalytic center, which are about 18 Å away. This indicates a new strategy to encode extra efficiency within other members of this enzyme family. Comparison of the 3D structure of the native and superefficient mutant enzymes does not reveal any substantial difference, suggesting that the increased activity must likely be ascribed to the dynamical properties of the two enzymes [76]. This hypothesis is in line with a recent molecular dynamics simulation study which demonstrated that the loop proximal to the active site is more flexible in the mutant than in the native enzyme [77], and with a series of molecular dynamics simulation studies which have shown mechanical coupling between the two subunits capable affecting the motion of the loops surrounding the active site [78, 79].

## Conclusions

Enzymes which are perfect from a chemical point of view have second-order catalytic rates which are limited by diffusion. Recent work has demonstrated that it is possible to engineer superefficient mutants by increasing enzyme-substrate association and leaving unaltered the already perfect active-site machinery. In the case of Cu, Zn SOD, this strategy has made it possible develop mutants with $k_{cat}/k_M$ of $1.7 \cdot 10^{10}$ $M^{-1}s^{-1}$, the highest catalytic rate ever reported for any enzyme.


1 Smoluchowski S. H. (1918) Versuch einer mathematischen Theorie der koagulationskinetik kolloider Losungen. Z. Phys. Chem. **92:** 129–168

2 Northrup S. H. and Erickson H. P. (1992) Kinetics of protein-protein association explained by Brownian dynamic computer simulation. Proc. Natl. Acad. Sci. USA **89:** 3338–3342

3 Schreiber G. and Fersht A. R. (1996) Rapid, electrostatically assisted association of proteins. Nat. Struct. Biol. **3:** 427–431

4 Stone R. S., Dennis S. and Hofsteenge J. (1989) Quantitative evaluation of the contribution of ionic interaction to the formation of thrombin-hirudin complex. Biochemistry **28:** 6857–6863

5 Jeltsch A. and Pingoud A. (1998) Kinetic characterization of linear diffusion of the restriction endonuclease EcoRV on DNA. Biochemistry **37:** 2160–2169

6 Sergi A., Ferrario M., Polticelli F., O'Neill P. and Desideri A. (1994) Comparison of simulated and experimental superoxide-superoxide dismutase association rate for six different natural variants. J. Phys. Chem. **88:** 10554–10557

7 Koppenol W. H. (1981) The physiological role of the charge distribution on superoxide dismutase. In: Oxygen and Oxyradicals in Chemistry and Biology, pp. 671–674, Rodgers M. A. J. and Powers E. L., (eds.), Academic Press, New York

8 Von Hippel P. H. and Berg O. G. (1989) Facilitated target location in biological systems. J. Biol. Chem. 264: 675–678

9 Riggs A. D., Bourgeois S. and Cohn M. (1970) The lac repressor-operator interaction. 3. Kinetic studies. J. Mol. Biol. **53:** 401–417

10 Jack W. E., Terry B. J. and Mordrich P. (1982) Involvement of outside DNA sequences in the major kinetic path by which EcoRI endonuclease locates and leaves its recognition sequence. Proc. Natl. Acad. Sci. USA **79:** 4010–4014

11 Ricchetti M., Metzeger W. and Heumann H. (1988) One-dimensional diffusion of *Escherichia coli* DNA-dependent RNA polymerase: a mechanism to facilitate promoter location. Proc. Natl. Acad. Sci. USA **85:** 4610–4614

12 Nardone G., George J. and Chirikijan J. G. (1986) Differences in the kinetic properties of BamHI endonuclease and methylase with linear DNA substrates. J. Biol. Chem. **261:** 12128–12133

13 Dowd D. R. and Lloyd R. S. (1990) Biological significance of facilitated diffusion in protein-DNA interactions. Applications to T4 endonuclease V-initiated DNA repair. J. Biol. Chem. **265:** 3424–3431

14 Herendeen D. R., Kassavetis G. A. and Geidusschek P. E. (1992) A transcriptional enhancer whose function imposes a requirement that proteins track along DNA. Science **256:** 1298–1303

15 Kelemen B. R. and Raines R. T. (1999) Extending the limits to enzymatic catalysis: diffusion of ribonuclease A in one dimension. Biochemistry **38:** 5302–5307

16 Surby M. A. and Reich N. O. (1996) Contribution of facilitated diffusion and processive catalysis to enzyme efficiency: implication for EcoRI restriction modification system. Biochemistry **35:** 2201–2208

17 Hasinoff B. B. (1982) Kinetics of acetylthiocholine binding to electric EEL acetylcholinesterase in glycerol/water solvents of increased viscosity. Evidence for a diffusion-controlled reaction. Biochim. Biophys. Acta **704:** 52–58

18 Nolte H. J., Rosenberry T. L. and Neuman E. (1980) Effective charge on acetylcholinesterase active sites determined from the ionic strength dependence of association rate constants with cationic ligands. Biochemistry **19:** 3705–3711

19 Sussman J. L., Harel M., Frolow F., Oefner C., Goldman A. and Silman I. (1991) Atomic structure of acetylcholinesterase from *Torpedo californica*: a prototypic acetylcholine-binding protein. Science **253:** 872–879

20 Ripoll D. R., Faerman C. H., Axelsen P. H., Silman I. and Sussman J.L. (1993) An electrostatic mechanism for substrate guid-

ance down the aromatic gorge of acetylcholinesterase. Proc. Natl. Acad. Sci. USA. **90:** 5128–5132
21 Shafferman A., Ordenlich A., Barak D., Kronan C., Ber R., Bino T. et al. (1994) Electrostatic attraction by surface charges does not contribute to the catalytiv efficiency of acetylcholinesterase. EMBO J. **13:** 3448–3455
22 Antosiewicz J., Mc Cammon J. A., Wlodek S. E. and Gilson M. K. (1995) Simulation of charge-mutant acetylcholinesterases. Biochemistry **34:** 4211–4219
23 Antosiewicz J., Wlodek S. E. and Mc Cammon J. A. (1995) Acetylcholinesterase: role of the enzyme's charge distribution in steering charged ligands toward the active site. Biopolymers **39:** 85–84
24 Christensen H., Martin M. T. and Waley S. G. (1990) $\beta$-Lactamases as fully efficient enzymes. Determination of all rate constants in acyl-enzyme mechanism. Biochem. J. **266:** 853–861
25 Matagne A. and Frere J. M. (1995) Contribution of mutant analysis to the understanding of enzyme catalysis: the case of class A $\beta$-lactamase. Biochim. Biophys. Acta **1246:** 109–127
26 Wade R. C., Gabdouline R. R., Ludemann S. K. and Lounnas V. (1998) Electrostatic steering and ionic tethering in enzyme-ligan binding: insights from simulations. Proc. Natl. Acad. Sci. USA **95:** 5942–5949
27 Hutletsky A., Couture F. and Levesque R. C. (1990) Nucleotide sequence and phylogeny of SHV-2 $\beta$-Lactamase. Antimicrob. Agents Chemother. **34:** 1725–1729
28 Noissinot M. and Levesque R. C. (1990) Nucleotide sequence of the PSE-4 carbenicillase gene and correlation with the *Staphylococcus aureus* PC1 $\beta$-lactamase crystal structure. J. Biol Chem. **265:** 1225–1230
29 Herzberg O. and Moult J. (1987) Bacterial resistance to $\beta$-lactam antibiotics: crystal structure of $\beta$-lactamase from *Staphylococcus aureus* PC1 at 2.5 Å resolution. Science **236:** 131–146
30 Ambler R. P., Coulson A. F., Frere J. M., Ghuysen J. M., Jaurin B., Joris B. et al. (1991) A standard numbering scheme for the class A $\beta$-lactamase. Biochem. J. **276:** 269–272
31 Schreiber G. and Fersht A. R. (1993) The interaction of barnase with its polypeptide inhibitor barstar studied by protein engineering. Biochemistry **32:** 5145–5150
32 Schreiber G. and Fersht A. R. (1996) Rapid, electrostatically assisted association of proteins. Nat. Struct. Biol. **3:** 427–431
33 Gabdoulline R .R. and Wade R. C. (1997) Simulation of the diffusional association of barnase and barstar. Biophys. J. **72:** 1917–1929
34 Blacklow S. C., Raines R. T., Lim W. A., Zamore P. D. and Knowles J. R. (1988) Triosephosphate isomerase catalysis is diffusion controlled. Biochemistry **27:** 1158–1167
35 Knowles J. R. (1991) Enzyme catalysis: not different, just better. Nature **350:** 121–124
36 Åqvist J. and Fothergill M. (1996) Computer simulation of the triosephosphate isomerase catalyzed reaction. J. Biol. Chem. **271:** 10010–10016
37 Raines R. T., Sutton E. L., Straus D. R., Gilbert W. and Knowles J. R. (1986) Reaction energetics of a mutant triosephosphate isomerase in which the active-site glutamate has been changed to aspartate. Biochemistry **25:** 7142–7154
38 Nickbarg E. B., Davenport R. C., Petsko G. A. and Knowles J. R. (1988) Triosephosphate isomerase: energetics of the reaction catalyzed by the yeast enzyme expressed in *Escherichia coli*. Biochemistry **27:** 5939–5947
39 Blacklow S. C. and Knowles J. R. (1990) How can a catalytic lesion be offset? The energetics of two pseudorevertant triosephosphate isomerases. Biochemistry **29:** 4099–4108
40 Cleland W. W. and Kreevoy M. M. (1994) Low-barrier hydrogen bonds and enzymic catalysis. Science **264:** 1887–1890
41 Cleland W. W., Frey P. A. and Gerlt J. A. (1998) The low barrier hydrogen bond in enzymatic catalysis. J. Biol. Chem. **273:** 25529–25532
42 Shan S. O. and Herschlag D. (1999) hydrogen bonding in enzymatic catalysis: analysis of energetic contributions. Methods Enzymol. **308:** 246–276
43 Zhang Z., Komives E. A., Sugio S., Blacklow S. C., Narayana N., Xuong N. H. et al. (1999) The role of water in the catalytic efficiency of triosephosphate isomerase. Biochemistry **38:** 4389–4397
44 Wade R. C., Gabdoulline R. R. and Luty B. A. (1998) Species dependence of enzyme-substrate encounter rates for triose phosphate isomerases. Proteins **31:** 406–416
45 Williams J. C. and McDermott A. E. (1995) Dynamics of the flexible loop of triosephosphate isomerase: the loop motion is not ligand gated. Biochemistry **34:** 8309–8319
46 Pompliano D. L., Peyman A. and Knowles J. R. (1990) Stabilization of a reaction intermediate as a catalytic device: definition of the functional role of the flexible loop in triosephosphate isomerase. Biochemistry **29:** 3186–3194
47 Sun J. and Sampson N. S. (1999) Understanding protein lids: kinetic analysis of active hinge mutants in triosephosphate isomerase. Biochemistry **38:** 11474–11481
48 Tainer J. A., Getzoff E. D., Richardson J. S. and Richardson D. C. (1983) Structure and mechanism of copper, zinc superoxide dismutase. Nature **306:** 284–287
49 Bannister J. V., Bannister W. H. and Rotilio G. (1987) Aspects of the structure, functions and applications of the superoxide dismutase. CRC Crit. Rev. Biochem. **22:** 111–180
50 Bertini I., Mangani S. and Viezzoli M. S. (1998) Structure and properties of copper/zinc superoxide dismutases. In: Advanced Inorganic Chemistry, pp. 127–250, Sykes A.G. (ed.), Academic Press, San Diego
51 Bordo D., Pesce A., Bolognesi M., Stroppolo M. E., Falconi M. and Desideri A. (2001) Copper-zinc superoxide dismutase in prokaryotes and eukaryotes. In: Handbook of Metalloproteins, Wieghardt K., Huber R., Poulos T. and Messerschmidt A. (eds) Wiley, London, in press
52 Djinovich K., Polticelli F., Desideri A., Rotilio G., Wilson K. J. and Bolognesi M. (1994) Crystallographic study of azide-inhibited bovine Cu,Zn superoxide dismutase. J. Mol. Biol. **240:** 179–183
53 Djinovich K., Battistoni A., Carrí M. T., Polticelli F., Rotilio G., Coda A. et al. (1994) Crystal structure of the cyanide-inhibited *Xenopus laevis* Cu,Zn SOD. FEBS Lett. **349:** 93–98
54 Leone M., Cupane A., Militello V., Stroppolo M. E. and Desideri A. (1998) Fourier transform infrared analysis of the interaction of azide with the active site of oxidized and reduced bovine Cu,Zn superoxide dismutase. Biochemistry **37:** 4459–4464
55 Cudd A. and Fridovich I. (1982) Electrostatic interactions in the reactions mechanism of bovine erythrocyte superoxide dismutase. J. Biol. Chem. **257:** 11443–11447
56 Rigo A., Viglino P. and Rotilio G. (1975) Polarographic determination of superoxide dismutase. Anal. Biochem. **68:** 1–8
57 Getzoff E. D., Tainer J. A., Weiner P. K., Kollman P. A., Richardson J. S. and Richardson D. C. (1983) Electrostatic recognition between superoxide and copper zinc superoxide dismutase. Nature **306:** 287–290
58 Klapper I., Hagstrom R., Fine R., Sharp K. and Honig B. (1986) Focusing of electric fields in the active site of Cu-Zn superoxide dismutase: effects of ionic strength and amino-acid modification. Proteins **1:** 47–59
59 Desideri A., Falconi M., Polticelli F., Bolognesi M., Djinovic K. and Rotilio G. (1992) Evolutionary conservativeness of electric field in the Cu,Zn superoxide dismutase active site. Evidence for co-ordinated mutation of charged amino acid residues. J. Mol. Biol. **223:** 337–342
60 O'Neill P., Davies S., Calabrese L., Capo C., Marmocchi F., Natoli G. et al. (1988) The effects of pH and various salts upon the activity of a series of superoxide dismutases. Biochem. J. **251:** 41–46

61 Sharp K., Fine R. and Honig B. (1987) Computer simulations of the diffusion of a substrate to an active site of an enzyme. Science **236:** 1460–1463
62 Allison S. A., Bacquet R. J. and McCammon J. A. (1988) Simulation of the diffusion-controlled reaction between superoxide and superoxide dismutase. II. Detailed models. Biopolymers **27:** 251–269
63 Sines J. J., Allison S. A. and McCammon J. A. (1990) Point charge distributions and electrostatic steering in enzyme/substrate encounter: Brownian dynamics of modified copper/zinc superoxide dismutases. Biochemistry **29:** 9403–9412
64 Beyer W. F., Fridovich I., Mullenbach G. T. and Hallewell R. (1987). Examination of the role of arginine-143 in the human copper and zinc superoxide dismutase by site-specific mutagenesis. J. Biol. Chem. **262:** 11182–11187
65 Fisher C. L., Cabelli D. E., Tainer J. A., Hallewell R. A. and Getzoff E. D. (1994) Role of Arg143 in the electrostatics and mechanism of a Cu,Zn superoxide dismutase: computational and experimental evaluation by mutational analysis. Proteins **19:** 24–34
66 Getzoff E. D., Cabelli D. E., Fisher C. L., Parge H. E., Viezzoli M. S., Banci L. et al. (1992) Faster superoxide dismutase mutants designed by enhancing electrostatic guidance. Nature **358:** 347–351
67 Polticelli F., Bottaro G., Battistoni A., Carrí M. T., Dijnovic-Carugo K., Bolognesi M. et al. (1995) Modulation of the catalytic rate of Cu,Zn superoxide dismutase in single and double mutants of conserved positively and negatively charged residues. Biochemistry **34:** 6043–6049
68 Polticelli F., Battistoni A., Bottaro G., Carrí M. T., O'Neill P., Desideri A. et al. (1994) Mutation of Lys120 and Lys134 drastically reduces the catalytic rate of Cu,Zn superoxide dismutase. FEBS Lett. **352:** 76–78
69 Polticelli F., Battistoni A., O'Neill P., Rotilio G. and Desideri A. (1998) Role of the electrostatic loop charged residues in Cu,Zn superoxide dismutase. Protein Sci. **7:** 2354–2588
70 Pesce A., Capasso C., Battistoni A., Folcarelli S., Rotilio G., Desideri A. et al. (1997) Unique structural features of the monomeric Cu,Zn superoxide dismutase from Escherichia coli, revealed by X-ray crystallography. J. Mol. Biol. **274:** 408–420
71 Stroppolo M. E., Sette M., O'Neill P., Polizio F., Cambria M. T. and Desideri A. (1998) Cu,Zn superoxide dismutase from *Photobacterium leiognathi* is an hyperefficient enzyme. Biochemistry **37:** 12287–12292
72 Pesce A., Battistoni A., Stroppolo M. E., Polizio F., Nardini M., Kroll J. S. et al. (2000) Functional and crystallographic characterization of *Salmonella typhimurium* Cu,Zn superoxide dismutase coded by the sodCI virulence gene. J. Mol. Biol. **302:** 465–478
73 Folcarelli S., Battistoni A., Falconi M., O'Neill P., Rotilio G. and Desideri A. (1998) Conserved enzyme-substrate electrostatic attraction in prokaryotic Cu,Zn superoxide dismutases. Biochem. Biophys. Res. Commun. **244:** 908–911
74 Folcarelli S., Venerini F., Battistoni A., O'Neill P., Rotilio G. and Desideri A. (1999) Toward the engineering of a super efficient enzyme. Biochem. Biophys. Res. Commun. **256:** 425–428
75 Stroppolo M. E., Pesce A., Falconi M., O'Neill P., Bolognesi M. and Desideri A. (2000) Single mutation at the intersubunit interface confers extra efficiency to Cu,Zn superoxide dismutase. FEBS Lett. **483:** 17–20
76 Stroppolo M. E., Pesce A., D'Orazio M., O'Neill P., Bordo D., Rosano C. et al. (2001) Single mutations at the subunit interface modulate copper reactivity in *Photobacterium leiognathi* Cu,Zn superoxide dismutase. J. Mol. Biol. **308:** 555–563
77 Falconi M., Stroppolo M. E., Cioni P., Sergi A., Ferrario M. and Desideri A. (2001) Dynamics-function correlation in *Photobacterium leiognathi* Cu,Zn superoxide dismutase: a spectroscopic and molecular dynamics simulation study. Biophys. J. **80:** 2556–2567
78 Falconi M., Gallimbeni R. and Paci E. (1996) Dimer asymmetry in superoxide dismutase studied by molecular dynamics simulation. J. Comput. Aided Mol. Des. **10:** 490–498
79 Chillemi G., Falconi M., Amadei A., Zimatore G., Desideri A. and Di Nola A. (1997) The essential dynamics of Cu, Zn superoxide dismutase: suggestion of intersubunit communication. Biophys. J. **73:** 1007–1018
80 Nicholls A., Sharp K. A. and Honig B. (1991) Protein folding and association: insights from the interfacial and thermodynamic properties of hydrocarbons. Proteins **11:** 281–296